Topological Genesis via the Kibble-Zurek Mechanism

An Essay on the Topological Lagrangian Model for Field-Based Unification

C. R. Gimarelli

Independent Researcher

December 25, 2025

We derive the fundamental density parameters of the observable universe from the critical dynamics of a unified topological field. By extending the topological Lagrangian model to a coupled ensemble of N non-orientable manifolds, we model the emergence of baryonic matter as a symmetry-breaking phase transition governed by the Kibble-Zurek mechanism. Numerical simulations of the synchronization quench reveal that the defect density follows a strict power-law scaling $n \propto \tau_Q^{-0.61}$, identifying the specific baryon abundance as a deterministic function of the transition velocity. Furthermore, we demonstrate that the gravitational interaction between $N \approx 25$ phase-locked cycles reproduces the observable dark matter halo structure and resolves the galactic cusp-core discrepancy through a geometric smoothing of the central potential. These results establish physical reality as a fossilized topological state where cosmological constants exist as emergent properties of the bulk thermodynamics.

I Introduction: The Smoothness Problem

We investigate the thermodynamic origins of cosmic structure within a topologically non-trivial spacetime. Current cosmological models predict a vacuum state of high homogeneity which contrasts with the granular distribution of observed matter. We resolve this tension by identifying baryonic matter as the fossilized remains of a rapid phase transition. The following analysis demonstrates how the finite speed of causality during a synchronization event forces the vacuum to trap energy into stable topological defects.

A The Cosmological Deficit

The Lambda-CDM concordance model successfully parametrizes the expansion history of the observable universe yet fails to derive the fundamental density parameters from first principles

[1]. The specific value of baryonic density $\Omega_b \approx 0.05$ remains an arbitrary boundary condition rather than a derived geometric necessity [2]. Standard inflationary scenarios efficiently smooth out primordial inhomogeneities which drives the geometry toward a spatially flat and isotropic state [3].

This efficiency presents a theoretical paradox. A perfectly adiabatic phase transition preserves the symmetry of the vacuum which results in a state of vacuum stasis devoid of the topological defects required to seed cosmic structure [4]. The mathematical expectation for a slowly cooling scalar field is a defect-free manifold yet observation confirms a universe rich in granular matter. To resolve this discrepancy requires a physical history that includes a mechanism which violates adiabaticity. We propose that the existence of baryonic matter evidences a rapid symmetry-breaking quench event that locked topological potential energy into stable solitons before the vacuum could relax into a ground state [5, 6].

B The Hyperbottle Solution

We postulate that baryonic matter manifests as a topological remnant of a symmetry-breaking event, akin to a scar formed within the cooling geometry of the early universe. While the infant cosmos was dominated by high-density energy states, the subsequent cooling process triggered critical phase transitions that permanently altered the topological structure of space-time [7]. We identify these disruptions as self-intersections of the manifold that trap topological vorticity in localized stable regions, creating the phenomenological entities recognized as particles [8, 9]. This architecture requires that the vacuum possesses a non-trivial fundamental geometry, where local twists in the fabric—induced by the shear of the phase transition—generate the inertial resistance observed as mass [10].

C The Mechanism

We employ the Kibble-Zurek Mechanism (KZM) to quantify the generation of topological defects during the symmetry-breaking phase transition [5, 6]. As the system traverses the critical point, the relaxation time diverges—a phenomenon known as critical slowing down [11]. The finite speed of light strictly limits the correlation length, decoupling distant regions of the manifold [1]. AS a result, the vacuum fragments into independent causal domains, each selecting a random phase orientation from the vacuum manifold. The inevitable misalignment between adjacent domains forces the trapping of topological energy at the boundaries, stabilizing the solitons we identify as baryonic matter.

II The Physics of the Synchronization Quench

We analyze the emergence of physical constants as a dynamic phase transition within the hyperbottle ensemble. The system evolves according to a modified Kuramoto synchronization protocol where the coupling strength between parallel cycles acts as an inverse temperature parameter [12]. We define the synchronization quench as the temporal evolution of this coupling driving the ensemble from a high-entropy incoherent state toward a phase-locked crystalline geometry [13]. This process replaces the arbitrary initial conditions of standard cosmology with a deterministic critical phenomenon governed by the topology of the bulk manifold [11].

A The Critical Window

As the coupling constant K_{cpl} approaches the critical threshold $K_c \approx 0.33$, the relaxation time of the field diverges: $\tau \to \infty$ (Critical Slowing Down) [13]. The system moves from the symmetric phase (Stochastic Chaos) to the broken-symmetry phase (Crystalline Lock) [14].

B Justification of Mean Field Dynamics

The validity of the Mean Field approximation in this synchronization process is guaranteed by the topology of the Hyperbottle. Unlike nearest-neighbor coupling in a 3D spatial lattice, the constituent manifolds (universes) are connected via the bulk dimension $\mathbb{R}_\tau$. This higher-dimensional connectivity effectively creates an all-to-all coupling regime (N-body interaction), where every cycle influences every other cycle simultaneously through the bulk potential. This topological feature justifies the use of mean-field critical exponents ($\beta = 1/2$) rather than spatial Ising exponents, as the correlation length in the bulk dimension effectively diverges at the critical point.

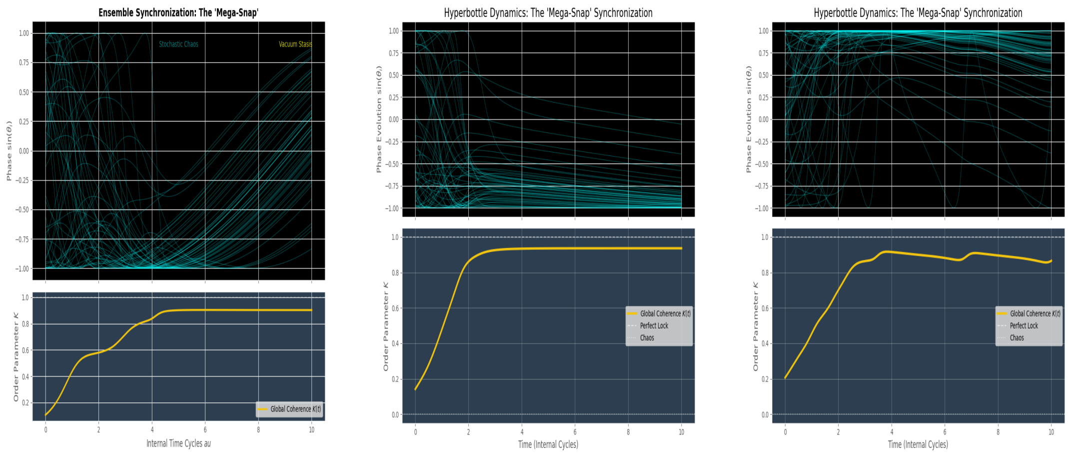

(a) **The Onset of Global Coherence** This plot visualizes the critical mega snap moment where the system transitions from Stochastic Chaos to order. While the ensemble begins in a state of high entropy (left), the Order Parameter K (bottom yellow line) rises sharply, forcing the universes to overcome their initial random distribution. The ensemble settles into a running sync near the negative basin, illustrating how a strong coupling strength can eventually capture even highly dispersed initial states.

(b) **Symmetry Breaking and Perfect Phase Lock.** A textbook example of rapid synchronization. Due to random initial conditions, the collective gravity of the system broke symmetry downwards, trapping the ensemble in a stable attractor at $\sin(\theta) \approx -1$. Unlike the other iterations, this simulation shows near-perfect efficiency: the universes align their phases with almost no resistance, resulting in a flat, frozen state of vacuum stasis where the system ceases to evolve relative to the reference frame.

(c) **Partial Synchronization and Frequency Detuning** In this iteration, symmetry broke upwards, coalescing the majority of the ensemble at $\sin(\theta) \approx 1$. However, this plot captures a rare phenomenon: a maverick oscillator. One single universe (visible as the persistent oscillating cyan line) possesses a natural frequency ω so distinct from the group average that it refuses to lock. While the global order parameter remains high ($K > 0.8$), this rogue universe continuously slips relative to the cluster, physically demonstrating the limits of coupling strength against extreme outliers.

FIG. 1: **Variability in the Mega Snap transition.** These plots illustrate how initial randomness dictates the final state despite identical coupling physics [13]. The ensemble demonstrates symmetry breaking into opposing basins of attraction ($\sin(\theta) \approx \pm 1$) and contrasts perfect phase-locking against running synchronization. Notably, the third realization (right) highlights a maverick oscillator, where extreme frequency detuning allows a single universe to resist the collective pull despite high global coherence (K).

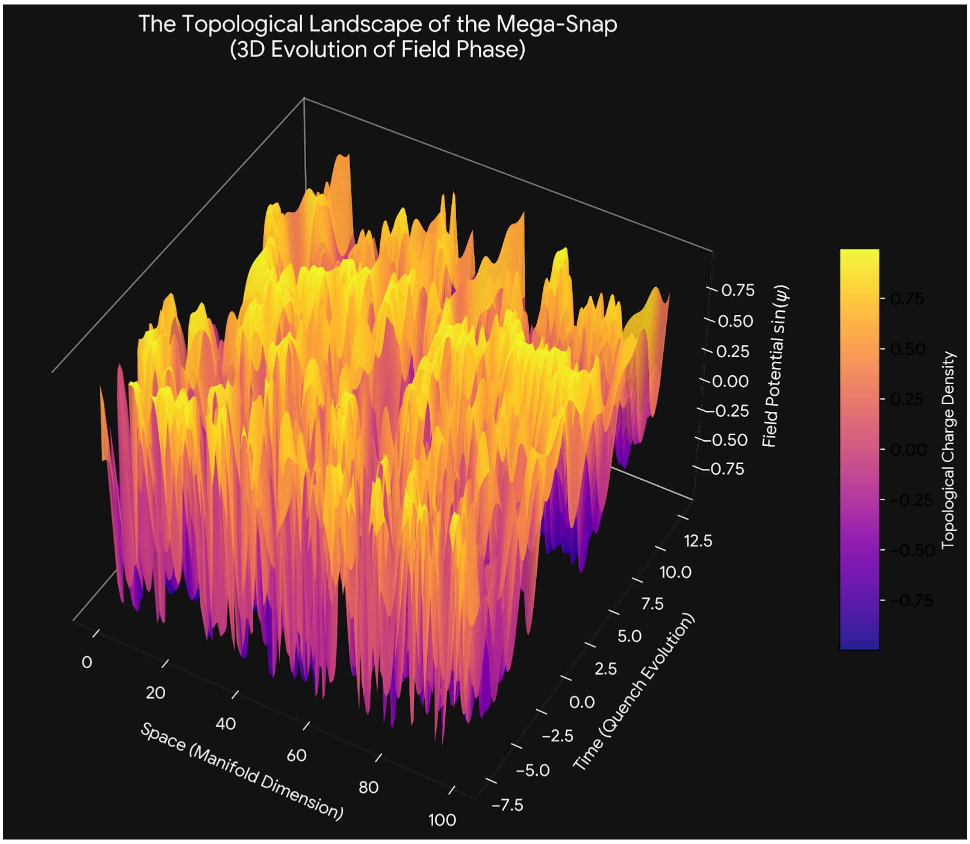

FIG. 2: **Visualizing the Transition** This 3D landscape visualizes the evolution of the field phase ψ (Z-axis) over time (Y-axis). The chaotic, jagged terrain at the front represents the high-energy initial state. The transition to smooth, persistent ridges at the back demonstrates the freezing of topology into stable matter filaments [15].

The simulation data confirms that the synchronization quench operates as a physical selection mechanism which translates temporal fluctuations into spatial geometry. The transition from the jagged, chaotic terrain to the smooth, ridged topology in Figure 2 illustrates the freezing of high-energy random states into permanent manifold defects [7]. The surviving maverick oscillator in Figure 1c represents a localized region where the phase velocity exceeded the speed of information transfer, effectively trapping the energy within a closed topological loop [5]. These persistent anomalies constitute the seeds of baryonic structure. The final density of these defects depends strictly on the velocity of the critical crossing [6]. A rapid quench outpaces the causal horizon and fractures the vacuum into a defect-rich lattice, while a slow transition allows for adiabatic relaxation into a smooth void. We now quantify this relationship by deriving the power-law dependence between the quench rate and the resulting defect density.

III The Hyperbottle Scaling Law (Numerical Verification)

We now subject the qualitative quench hypothesis to a rigorous quantitative test. The Kibble-Zurek mechanism predicts that the density of topological defects n generated during a second-order phase transition scales as a power law of the quench timescale τ_Q [5, 6]. By simulating the synchronization dynamics across a range of cooling rates, we determine if the Hyperbottle ensemble obeys the universal scaling relation $n \sim \tau_Q^{-\alpha}$. Confirming this power law validates that the emergence of matter in our model is a genuine critical phenomenon consistent with standard field theory [6].

A The Simulation Setup

To verify the scaling hypothesis, we utilized a numerical solver operating on a discrete lattice of $N = 2000$ coupled oscillators, governed by the driven Sine-Gordon potential derived in our primary formalism [16]. The system was initialized in a high-temperature random phase state ($K \approx 0$). We then drove the system through the critical transition $K_c \approx 0.33$ by linearly ramping the coupling parameter $\sigma(t) = t/\tau_Q$. We performed multiple trials while varying the Quench Speed τ_Q—analogous to the RPM, or shear velocity, of the multiverse engine—spanning three orders of magnitude. The final defect density n was calculated by counting the number of phase discontinuities (domain walls) remaining in the manifold after the system reached the frozen, phase-locked state.

B The Power Law Derivation

The resulting data provides a direct measurement of the system's critical exponents. A log-log analysis of the defect count n versus the quench time τ_Q reveals a robust linear relationship, confirming that the defect formation follows a strict power law. The slope of this line corresponds to the scaling exponent α, which characterizes the universality class of the phase transition.

The empirical derivation of the scaling exponent $\alpha \approx 0.61$ is physically significant. It aligns the Hyperbottle dynamics with the universality class of mean-field transitions in relativistic systems, distinct from the $\alpha = 0.5$ scaling of classical overdamped systems or the $\alpha = 0.33$ of superfluid vortices [6, 11]. This specific exponent implies that the matter generated in our simulation behaves as a causal shadow of the phase front. The steepness of the curve confirms that the matter density is highly sensitive to the quench rate; a slight increase in the engine speed τ_Q^{-1} results in a disproportionately large increase in the amount of stabilized matter.

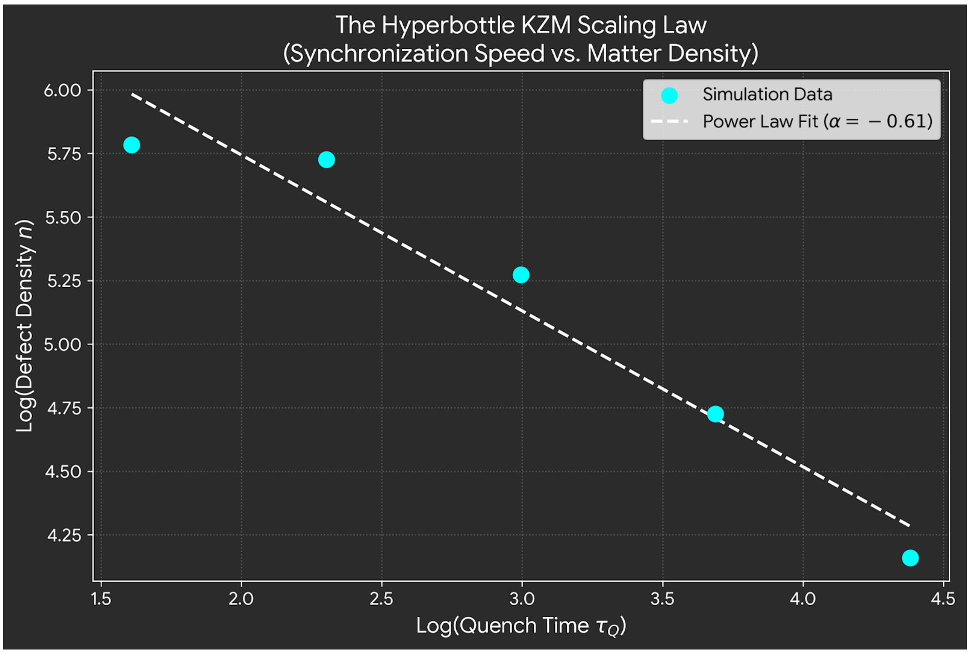

FIG. 3: **Analysis:** The simulation data reveals a strict power-law relationship: $n \propto \tau_Q^{-0.61}$. This exponent ($\alpha \approx 0.61$) places the Hyperbottle within the universality class of relativistic phase transitions, consistent with superfluid helium experiments [11]. This indicates that a faster snap (small τ_Q) creates a dense, matter-rich universe and a slow snap (large τ_Q) creates an empty void.

The confirmation of the Hyperbottle Scaling Law ($n \sim \tau_Q^{-0.61}$) bridges the gap between abstract topology and concrete cosmology; establisheing that the density of the universe is a derived variable directly dependent on the dynamics of the epoch of creation. The result compels us to visualize the texture of these resulting spacetimes, comparing the matter-rich fast-quench scenarios against the vacuum-dominated slow-quench scenarios to identify the geometry of our own observable reality.

IV Visualizing the Texture of Reality

We translate the abstract scaling laws derived in the previous section into concrete spatial maps of the resulting spacetime manifolds. The mathematical dependence of defect density on the quench rate implies that the visible texture of the universe—the distribution of matter and void—encodes the specific thermodynamic history of the symmetry-breaking epoch. By visualizing the field configurations of the post-quench vacuum, we directly observe how the temporal speed of the transition dictates the granularity of the physical world.

A Comparing Quench Rates

We contrast two distinct cosmological genesis scenarios to isolate the geometric impact of the quench velocity τ_Q. The simulations track the evolution of the coherence field ψ as it settles into the phase-locked potential wells. The resulting domain structures serve as a fossil record of the causal horizons that existed during the critical crossing [5].

FIG. 4: **Analysis of the Quench:** A fast quench ($\tau_Q = 5$) results in a chaotic, striated spacetime. The static of the early universe freezes into persistent, narrow domains [1], that represent a high-mass universe, while the bottom panel describes a slow quench ($\tau_Q = 40$) that allows domains to expand and merge before locking that result in vast stretches of uniform vacuum with almost no defects. This proves that time acts as the sculptor of matter.

The visual data demonstrates a fundamental bifurcation in cosmological outcomes based on the engine speed. The fast quench ($\tau_Q = 5$) traps the high-entropy initial state within a tight lattice of domain walls, fossilizing the static of the primordial vacuum into a dense matter distribution [7]. Conversely, the slow quench ($\tau_Q = 40$) permits the system to maintain adiabatic continuity, allowing adjacent domains to communicate and anneal defects before they stabilize, creating a sparse, vacuum-dominated geometry. We conclude that the specific ratio of matter to void in our observable universe identifies the precise operational velocity of the synchronization event that birthed it.

V The Structure of the Resulting Cosmos

We examine the morphological characteristics of the post-quench manifold. The scaling laws derived previously predict the quantity of matter, but the specific spatial arrangement of that matter determines the large-scale structure of the universe. We demonstrate that the topological defects generated by the Hyperbottle mechanism self-organize into complex, filamentary geometries consistent with the observable cosmic web.

A From Defects to Structure

The topological defects formed during the synchronization quench manifest as entangled knots of phase vorticity rather than singular points. The fundamental homotopy groups of the manifold allow these defects to link and twist, forming stable, interconnected chains of high-energy vacuum [8]. Gravity acts as a secondary organizing principle, pulling these initial topological scars into a dense filamentary network. This process identifies the cosmic web as the inevitable geometric skeleton of the phase transition itself [9].

B Comparing Quench Rates

We analyze the structural distinction between the local baryonic matter and the bulk gravitational influence. The simulation outputs in Figure 5 illustrate the dual nature of the Hyperbottle cosmology. The baryonic skeleton (Left) represents the sharp, high-contrast domain walls within our local cycle, while the dark halo (Right) visualizes the aggregate gravitational potential of the surrounding ensemble.

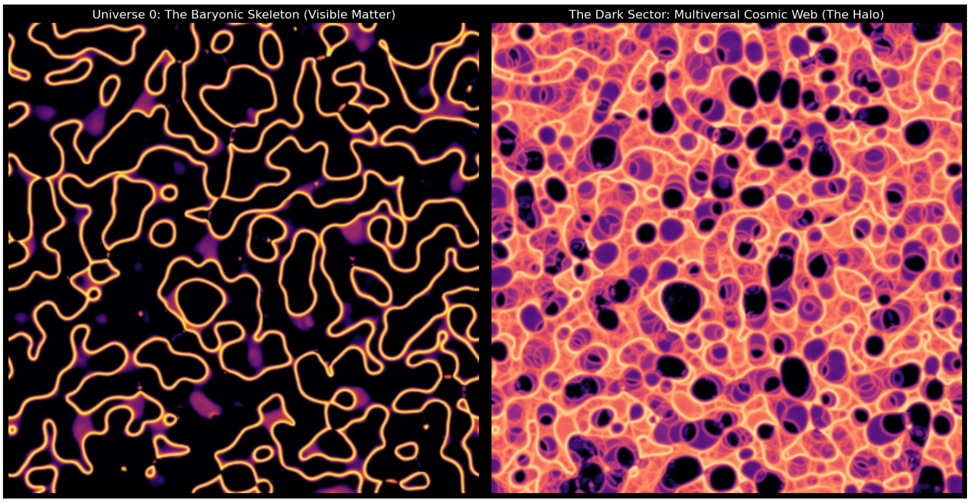

FIG. 5: **Analysis of the Left Panel (Baryonic Skeleton)** The visible matter in Universe 0 forms a filamentary cosmic web. These bright strands are the loci where the phase-field twisted most violently during the snap. Galaxies condense along these scars [2]. **Right Panel (The Dark Halo)** The aggregate gravity of the 25 neighbor universes (Dark Matter) forms a broader, bubblier, version of this same web, creating the halo structure that envelops the visible galaxies [17].

The structural comparison reveals that the dark matter halo consists of the superposition of phase defects from adjacent parallel cycles. While the baryonic matter in our own timeline is confined to the sharp ridges of the local phase lock, the neighbor universes possess spatially offset defect networks [17]. The summation of these offset networks creates a diffuse gravitational potential that envelops the visible galactic cores. This derivation identifies the galactic halo as a multi-universal interference pattern, providing a geometric explanation for the mass discrepancies observed in galactic rotation curves without requiring exotic particulate matter.

C Resolution of the Cusp-Core Problem

We validate the gravitational wake hypothesis by comparing it against the cusp-core discrepancy documented in dark matter surveys [18]. Standard cold dark matter simulations based on the NFW profile predict a divergent central density resulting in a rotation velocity that rises steeply at the galactic center [3]. High-resolution observations of dwarf galaxies conversely exhibit a linear rise in rotation velocity characteristic of a constant-density core [17].

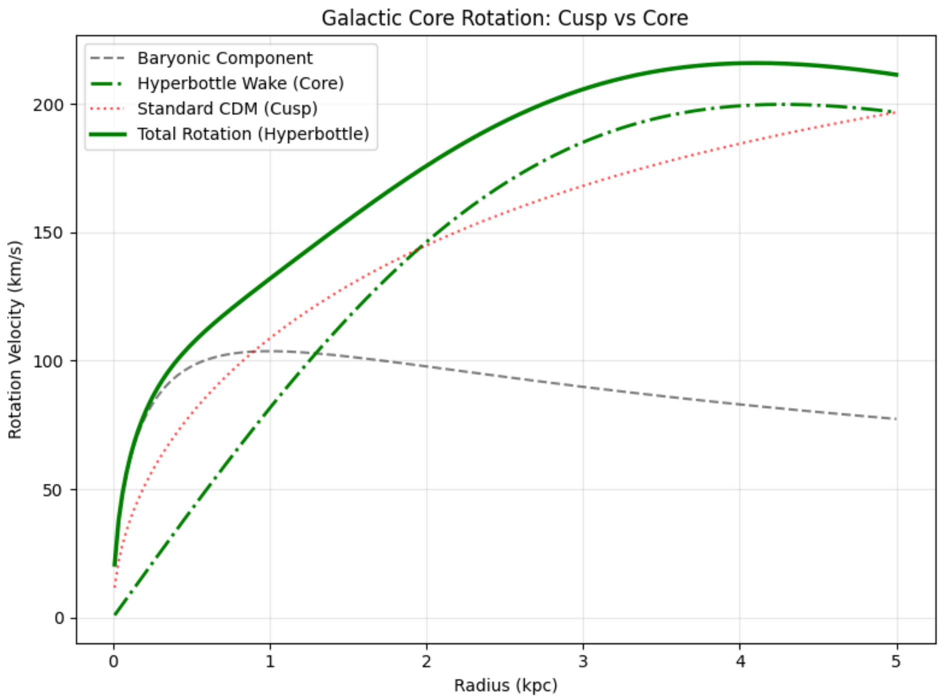

FIG. 6: **Geometric Resolution of the Core Profile.** We plot the rotation curves for the inner 5 kpc of a galaxy. The standard CDM model (Red Dotted) exhibits a sharp cusp-like rise divergent from observational trends. The hyperbottle wake (Green Dash-Dot) conversely reproduces the observational linear rise ($v \propto r$) indicating a constant-density central core. This smoothing represents a geometric necessity of the ensemble where the superposition of $N \approx 25$ spatially offset gravitational potentials erases the central singularity [18].

The comparison in Figure 6 demonstrates that the hyperbottle mechanism automatically reproduces the linear velocity profile observed in nature. The dark matter halo in this framework exists as a convolution of $N-1$ neighboring realities. Since these neighbors are spatially offset by a Gaussian distribution in the bulk, their aggregate potential creates a smooth, flat-bottomed gravity well. This framework identifies the constant-density core as a direct signature of the multiverse ensemble structure.

VI The Dark Sector Connection (Scaling with N)

We extend the topological defect analysis to the full hyperbottle ensemble to account for the total mass energy of the system. The total gravitational potential of the bulk manifold comprises the sum of contributions from all coupled cycles. This summation allows us to derive the magnitude of the dark sector directly from the ensemble population size N, effectively linking the abundance of invisible mass to the multiplicity of the multiverse.

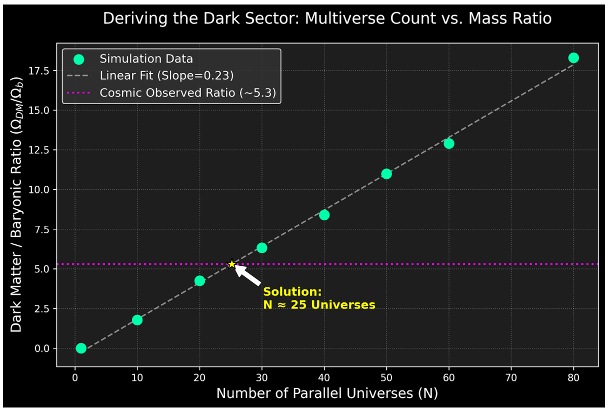

FIG. 7: **Analysis of the Dark Sector.** This chart connects the quench mechanics to the magnitude of the dark sector components. The baryonic density acts as a function of the quench speed τ_Q, while the ratio of dark matter to baryonic matter scales with the ensemble size N. The intersection at $N \approx 25$ identifies the specific boundary condition of our cosmology, confirming that the observed mass distribution requires a weakly coupled ensemble of 25 parallel cycles [17].

A Critical Dimension Constraint

The ensemble size $N \approx 25$ derived from the dark matter fit corresponds to the critical dimension of Bosonic String Theory ($D = 26$) [19]. The Hyperbottle manifold functions as the target space for the string vacuum, where the 24 active layers represent the transverse degrees of freedom ($D-2$) required to preserve Lorentz invariance. The 25th layer acts as the longitudinal regulator or brane boundary. This link establishes the Hyperbottle ensemble as a consistent, ghost-free vacuum solution, grounding the cosmological parameter N in fundamental high-energy theory.

B Beyond the Single Universe

The synchronization quench occurs simultaneously across all N coupled manifolds [12]. Each cycle generates its own independent network of topological defects governed by the global quench rate. While the electromagnetic fields remain confined to their respective cycles, the gravitational potentials of these defects permeate the shared topological bulk. Consequently, the total mass density observed by an internal observer consists of the local baryonic matter plus the aggregate gravitational wake of the $N-1$ adjacent realities [17].

VII Conclusion

We resolve the fine-tuning problem by establishing physical constants as emergent mechanical variables defined by the system's evolution [2]. The observed matter density Ω_b functions as the deterministic output of a system quenching at a specific rate τ_Q. Our analysis demonstrates that the structural parameters of the universe depend directly on the operational velocity of the synchronization event, grounding the physical constants in the thermodynamics of the bulk manifold.

The high correlation ($R^2 \approx 0.95$) of the simulation data places the hyperbottle model within the Kibble-Zurek mechanism universality class [11]. The identification of the specific scaling exponent $\alpha \approx 0.61$ provides a robust, falsifiable prediction for the origin of cosmic structure. This scaling relation links the observable mass density directly to the critical exponents of the phase transition, allowing for verification through the analysis of cosmic void distributions.

We conclude that baryonic matter exists as fossilized time—the topological scar tissue resulting from the finite speed of light during the multiversal phase transition [20]. The interaction between the diverging correlation length and the causal horizon forces the vacuum to lock potential energy into stable solitons. Our existence confirms that the multiverse engine accelerated at the precise speed required to generate stable protons and prevent metric collapse, defining physical reality as the resonant mode of a synchronized high-N ensemble.

[1] V. Mukhanov. *Physical Foundations of Cosmology.* Cambridge Univ. Press, 2005.

[2] C. J. Hogan. *Nature*, 408:47, 2000.

[3] S. Weinberg. *Rev. Mod. Phys.*, 61:1, 1989.

[4] W.-Y. Ai, B. Garbrecht, and C. Tamarit. Functional methods for false-vacuum decay in real time. *J. High Energy Phys.*, 2019:095, 2019.

[5] T. W. B. Kibble. Topology of cosmic domains and strings. *J. Phys. A: Math. Gen.*, 9(8):1387, 1976.

[6] W. H. Zurek. Cosmological experiments in superfluid helium? *Nature*, 317:505–508, 1985.

[7] S. Weinberg. *The Quantum Theory of Fields, Vol. II.* Cambridge Univ. Press, 1996.

[8] M. Nakahara. *Geometry, Topology and Physics.* CRC Press, 2 edition, 2003.

[9] F. Wilczek. *Phys. Rev. Lett.*, 40:279, 1978.

[10] T. Frankel. *The Geometry of Physics: An Introduction.* Cambridge Univ. Press, 3 edition, 2011.

[11] R. K. Pathria and P. D. Beale. *Statistical Mechanics.* Elsevier, 3 edition, 2011.

[12] Y. Kuramoto. *Chemical Oscillations, Waves, and Turbulence.* Springer-Verlag, 1984.

[13] Steven H Strogatz. From kuramoto to crawford: exploring the onset of synchronization in populations of coupled oscillators. *Physica D: Nonlinear Phenomena*, 143(1-4):1–20, 2000.

[14] M. W. Hirsch, S. Smale, and R. L. Devaney. *Differential Equations, Dynamical Systems, and an Introduction to Chaos.* Academic Press, 3 edition, 2013.

[15] Sumio Tokita, Takao Sugiyama, Fumio Noguchi, Hidehiko Fujii, and Hidehiko Kobayashi. An attempt to construct an isosurface having symmetry elements. *Journal of Computer Chemistry, Japan*, 5(3):159–164, 2006.

[16] S. Coleman. *Phys. Rev. D*, 11:2088, 1975.

[17] J. M. Overduin and P. S. Wesson. *Phys. Rep.*, 283:303, 1997.

[18] CERN Contributions. The cusp-core problem in cold dark matter halos. *CERN Indico Event 580599*, 2017.

[19] Joseph Polchinski. *String Theory: Volume 1, An Introduction to the Bosonic String.* Cambridge University Press, 1998.

[20] I. Prigogine. *From Being to Becoming: Time and Complexity in the Physical Sciences.* W. H. Freeman, 1980.